2017 24th national and 2nd International Iranian Conference on Biomedical Engineering (ICBME), Amirkabir University of Technology, Tehran, Iran, 30 November - 1 December 2017

Incorporating a local speed map in the levelset function

With applications in liver segmentation

Marzieh Jandaghi[1], Amir Hossein Foruzan[1], SH Momeni-Masuleh[2]

[1]Biomedical Engineering Department, Faculty of Engineering, [2]Faculty of Science, Shahed University, Tehran, Iran.
m.jandaghi@shahed.ac.ir, a.forouzan@shahed.ac.ir, momeni@shahed.ac.ir

Yen-Wei Chen

Intelligent Image Processing Lab, College of Information Science and Engineering, Ritsumeikan University, Japan.
chen@ritsumei.ac.jp

***Abstract*—In this paper, we proposed a method for liver segmentation in CT-scan images that is based on geometric active contours. After reading an input image, we obtain an initial segmentation by an intensity-based technique. Then, we apply a dilation filter on the initial surface to obtain an incremental narrow volume around it. We divide this volume into smaller parts and we prepare the corresponding velocity field in each part individually. The initial surface evolves under the velocity field and this process iterates until convergence. We applied our method on 30 CT-scan datasets including healthy/patient people, and contrast-enhanced/low-contrast images. The average Dice and Jaccard indices were 0.91 and 0.84 respectively. Compared to the STACS algorithm, we improved Dice and Jaccard indices by 0.63 and 0.47.**

Keywords— Liver segmentation, Levelset function, STACS model, Medical image processing.

I. INTRODUCTION

Medical images contain anatomical information that physicians use for accurate diagnosis, treatment planning, and monitoring. Thus, their processing is vital to physicians.

Image segmentation is a branch of image processing that has several applications including measuring the volume of an organ and determining the location of a tumor. There are difficulties in segmentation of medical images such as image noise, partial volume effect (more than one tissue exists in a voxel) and image quality.

Segmentation of human liver in CT images is a difficult task due to image noise, PVE, shape variation and complex stochastic model of non-liver tissues [1].

Researchers have proposed several methods to resolve these problems. The active contour algorithm is a major image segmentation technique. In this technique, an initial curve (as the zero levelset of a higher dimension function) moves towards true edges of an organ influenced minimizing an energy function. Typical problems concerned with this method are initial settlement of the contour, controlling the energy function in noisy and low-contrast images, and definition of the boundary in complex shaped objects.

II. PREVIOUSE WORK

The energy function of an active contour contains internal and external forces. The internal force controls the contour to be smooth and the external force absorbs it towards high-gradient regions. Minimization of the energy function moves the curve to the edges of the image. Researchers classify active contours into parametric and geometric categories. Parametric active contours have problems with contour division and merging and their extension to higher dimensional spaces is tedious. Geometric active contours include edge-based and region-based techniques. In edge-based methods, we use edge information to expand the contour while we employ regional information in region-based category.

A. Chan-Vese Model

Chan and Vese proposed a popular model of region-based active contours. They called it Active Contours Without Edges (ACWE) [2]. This method computes the intensity difference between inside and outside of an initial contour and tries to move the levelset so that the inside and outside regions can be described by a simple intensity model. A fundamental assumption in ACWE is that the input image has homogenous textures inside and outside of the object. However, most medical images have complex statistical models and do not follow this assumption.

B. Hybrid level set models

To solve for inhomogeneous textures, Wang *et al.* suggested a hybrid levelset model [3]. The energy functional of this model was composed of three terms: global term, local term and regularization term. Since intensity of small regions is more homogeneous, this method uses local information to prepare its speed map. To prepare local information, a smoothing filter blurs an input image and they subtract the result from the original image. Then, they calculate the

978-1-5386-3609-1/17/$31.00 ©2017 IEEE

average of intensities inside and outside of the contour. In the blurred image, they subtract the intensities of inside and outside from the corresponding mean values and the integration of these differences makes the local energy term. The global term is the Chen-Vese energy term. The regularization term keeps the contour smooth. The algorithm gives a weight to local and global terms in the energy function. In inhomogeneous regions, they increase the weight of the local information with respect to the global one to compensate for texture variations.

C. STACS

Pluempitiwiriyawej *et al.* introduced a stochastic active contour scheme (STACS) to segment the heart from cardiac images [4]. This method is both an edge-based and a region-based technique. They included shape information to address problems concerned with low contrast images, papillary muscles and turbulent blood flow.

The energy function of STACS has four parts: the region-based, the edge-based, prior shape and smoothness terms. They assume that the input image contains an object and a background and describe their intensity models by two Gaussian density functions. The energy function maximizes the probability that the statistical model of the outside region is similar to the background and that of the inside region is identical to the object.

The edge-based term moves the contour to the edges of the images. The corresponding edge map is the magnitude gradient of the smooth image.

The prior shape term makes the shape of the contour like an ellipse since they assume that the profile of the heart is approximately elliptic. The regularization term controls smoothness and length of the contour.

In this paper, we propose a variation of the STACS to segment liver in CT images. We incorporate a local speed map to consider complex statistical model of non-liver tissues. In section 3, we explain the proposed method. The results are in section 4 and we discuss them in section 5. We conclude the paper in section 6.

III. THE PROPOSED METHOD

A. Preparing the initial contour

After reading an input image, a physician manually defines the region of interest (ROI) of liver to reduce the size of data and run-time of the code. If the size of 3D data is larger than 100 pixels, we decimate it to reduce memory requirements. To prepare the initial contour, we segment liver by the Narrow Band Thresholding algorithm (NBT) [5]. We apply a morphological erosion filter on the result to insure that the contour is inside the liver.

B. The local speed map

A speed map controls evolution of the contour. Human liver is in contact to several tissues with different intensity models. To consider complex stochastic model of non-liver tissues, we define the speed map locally. We define it in a narrow region around the current location of the contour. Thus, we decrease the run-time of our code well. Then, we divide this region into several sections. The sign of the speed map depends on statistical information of each section. A positive map evolves the contour and a negative map shrinks it. We model the intensity of liver inside the initial contour by a single Gaussian. If the intensity model of a section is similar to the liver's model, the contour will evolve in that section; otherwise, it will stop evolution. The similarity measure is the absolute difference between the mean intensity of the section and the mean intensity of the liver region. In (1), we define mean intensity of the A_i section.

$$\mu_{A_i} = \frac{\int_{A_i} I(x,y,z)\,dxdydz}{\int_{A_i} dxdydz}. \quad (1)$$

In (1), I(.) is the image intensity. We define the average of intensity inside liver (μ_L) by (2).

$$\mu_L = \frac{\int_{\Omega} I H(\phi(x,y,z))\,dxdydz}{\int_{\Omega} H(\phi(x,y,z))\,dxdydz}, \quad (2)$$

In (2), we define the levelset function by $\phi(.)$ and the heaviside function H(z) by (3).

$$H(z) = \begin{cases} 1, & if\ z \geq 0 \\ 0, & if\ z < 0 \end{cases}, \quad (3)$$

After we set the signs of all sections, we solve the differential equation corresponding to the levelset numerically. We define the speed map and solve the differential equation iteratively until convergence.

We represent the speed map mathematically by (4)-(6).

$$S = H(\phi)|k_0| - \left[1 - H(\phi) - \cup_{i=1}^{2N^2} H(\Delta\phi_i)\right]|k_0| + \cup_{i=1}^{2N^2} H(\Delta\phi_i)k_i. \quad (4)$$

$$k_i = |k_0|,\ if\ |\mu_L - \mu_{A_i}| \leq Threshold. \quad (5)$$

$$k_i = -|k_0|,\ if\ |\mu_L - \mu_{A_i}| > Threshold. \quad (6)$$

In (4)-(6), $k_0 = 1$ is a constant and $\Delta\phi_i$ is the incremental levleset in ith section.

To define sections, we divide the space around the current contour into N parts in the elevation direction (θ) and 2N parts in the azimuth direction (ϕ). Thus, there are $2N^2$ sections totally.

C. The energy function

The proposed energy function consists of smoothing and balloon terms.

$$\frac{\partial \varphi}{\partial t} = |\nabla\phi| \left[S + \mathrm{Div}\left(\frac{\nabla\phi(x,y)}{|\nabla\phi(x,y)|}\right)\right]. \quad (7)$$

We use the local speed map (S) as the balloon force and the $\mathrm{Div}\left(\frac{\nabla\phi(x,y)}{|\nabla\phi(x,y)|}\right)$ term as the classical smoothing term. We solve the differential equation in (7) numerically until it converges or number of iterations is more than a threshold.

We describe the steps of our method in Algorithm-I in more detail.

978-1-5386-3609-1/17/$31.00 ©2017 IEEE

Algorithm-I: Liver segmentation by the proposed method

Inputs: Liver CT image, number of divisions in the narrow volume (N), size of dilation structuring element (SE), number of iterations (K).

Step1. Segment liver in the input CT image by the NBT [5] method.

Iteration = 0.
Do
Step2. Dilate the resultant liver mask (using SE) to make the initial liver surface.

Step2. Dilate the initial surface to create an incremental volume. Divide the incremental volume into N parts in the elevation direction (Θ) and 2N parts in the azimuth direction (ϕ).

For i = 1 **to** N.
$\Theta_I = (i-1)\times\pi/N.$
$\Theta_F = i\times\pi/N.$
For j = 1 **to** N2.
$\phi_I = (j-1)\times 2\pi/N.$
$\phi_F = j\times 2\pi/N.$
Calculate the local speed map using (5) and (6).
End
End

Step3. Solve the differential equation in (7).
Iteration = Iteration + 1;
While Iteration < K

Output: Final liver mask.

IV. Results and Discussions

We implemented our code in MATLAB environment using a personal computer with an Intel Core i5 processor with 4GB memory. We evaluated our results by the Dice and Jaccard measures defined in (8) and (9).

$$D = \frac{2|M_{Auto}\cap M_{Ref}|}{|M_{Auto}|+|M_{Ref}|}. \quad (8)$$

$$J = \frac{|M_{Auto}\cap M_{Ref}|}{|M_{Auto}\cup M_{Ref}|}. \quad (9)$$

In (8) and (9), M_{auto} and M_{Ref} refer to segmentation by our method and manual segmentation respectively.

A. Experimental results on synthetic data

For quantitative evaluation of our method, we used a synthetic image. It contained a 30x30x30 cube inside a 50x50x50 blank image. We set intensities of the cube and background pixels as 1 and 0 respectively. We included varying levels of additive Gaussian noise to assess robustness of our method against noise as well. Table 1 shows the results of our algorithm using Dice and Jaccard indices. As is shown in Table 1, the results of our method do not change greatly when we increase the variance of noise. We also utilized synthetic data to examine sensitivity of our method to its parameters.

B. Experimental results on clinical data

We used CT images of healthy and patient men and women to evaluate our method as well. The dataset belonged to Osaka University, Japan and contained 30 abdominal images of the portal venous phase images. The resolution and size of images were 512×512×159 and 0.625×0.625×1.25 mm^3, respectively. University Ethics Committee approved the usage of the dataset. We show the results in Table 2 indicate the results of our method on OsakaID data.

TABLE I. SEGMENTATION RESULTS ON SYNTHETIC DATA.

Noise Level (variance)	0.1	0.2	0.3	0.4	0.5	variance
Dice	0.99	0.99	0.98	0.98	0.98	0.005
Jaccard	0.98	0.98	0.97	0.96	0.96	0.01

TABLE II. SEGMENTATION ON CLINICAL DATA

Data Number	ID02	ID10	ID15	ID16	ID18	variance
Dice	0.9	0.91	0.92	0.91	0.91	0.007
Jaccard	0.82	0.83	0.85	0.85	0.84	0.013

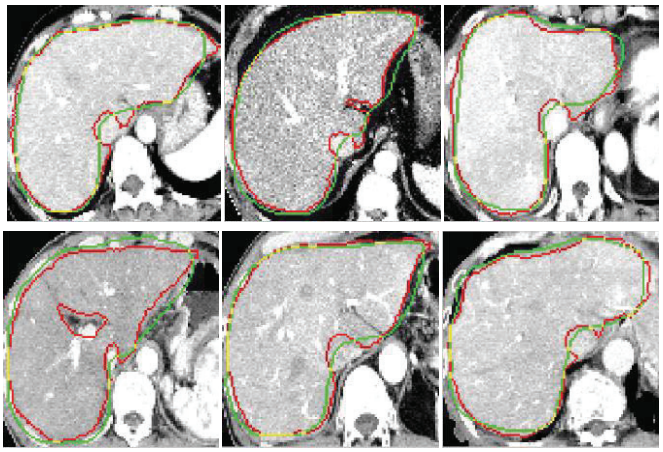

Fig. 1. Comparison of our method (green contour) and manual segmentation (red contour).

TABLE III. SEGMENTATION ON CLINICAL DATA

Data number	1	2	3	4	5	Variance
Dice	0.89	0.9	0.88	0.88	0.9	0.01
Jaccard	0.8	0.82	0.78	0.78	0.81	0.018

978-1-5386-3609-1/17/$31.00 ©2017 IEEE

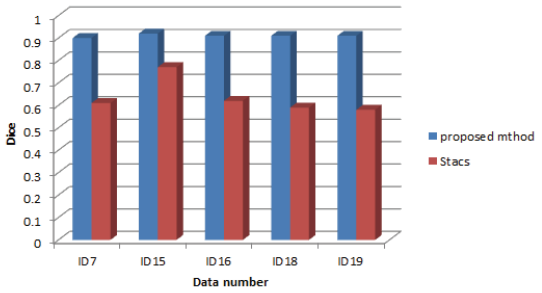

Fig. 2. Comparison of segmentation results by our method and STACS.

Since there is only a single object in the synthetic data, there is no problem concerned with leakage. If we consider the noise variance, we can conclude that our results are promising.

Average Dice and Jaccard measures were 0.91 and 0.84 respectively. Regarding Dice and Jaccard metrics, the standard deviations of our results were 0.013 and 0.023 respectively. In Table 3, we show segmentation results of our method using low contrast images. Average Dice index of low contrast images is 0.89 that is not very different from normal contrast enhanced data. It reveals that our method can be used to segment both contrast enhanced and non-contrasted images too. In Fig. 1, we compare our results with manual segmentation qualitatively.

We compared our method with recent (STACS) and conventional (Chan-Vese) levelset segmentation techniques (Fig. 2 and 3). As w show in Fig. 2, our method achieves higher measures compared to the STACS method. Regarding the Chan-Vese method, it leaks nearby organs while our method leaks much less. The proposed local speed map explains the reason why our method improves the results. Since it defines how the levelset expands more accurately. We improved segmentation results by the STACS and Chan-Vese methods by 0.628 and 0.55 averagely.

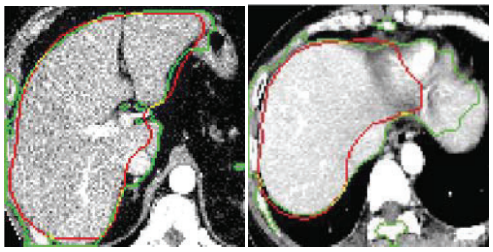

(a) (b)

Fig. 3. Comparison of segmentation results by our method and Chan-Vese. (a) OsakaID0018 (b) OsakaID0020. Red contour is our method. Green contour is Chan-Vese.

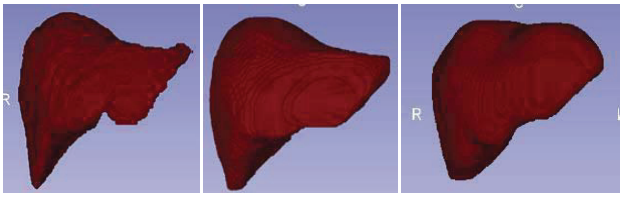

(a) (b) (c)

Fig. 4. Variations of our method to size of the structuring element (SE) in the dilation filter. (a) Manual segmentation. (b) Segmentation by our method using SE-size=1. (c) Segmentation by our method using SE-size=4.

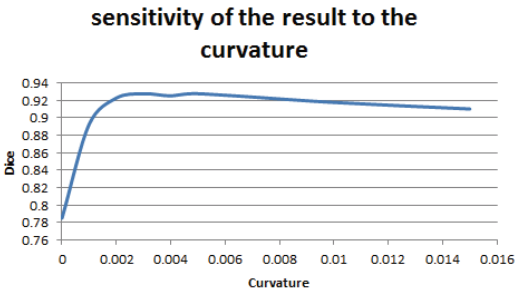

Fig. 5. Sensitivity of our method to variations of the curvature coefficient.

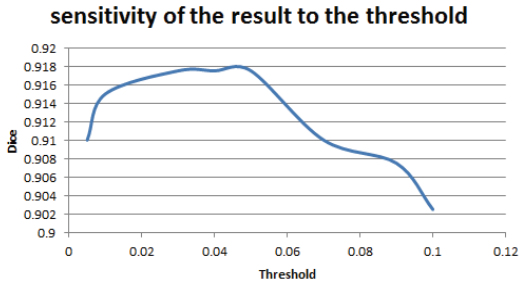

Fig. 6. Sensivity of our method to variations of the threshold (Eq. 5).

We evaluated sensitivity of our method to parameter variations (Fig. 4-6). In Fig. 5, we show variations of the results with respect to structuring element (SE) size. A large SE size makes the code to run faster and requires less memory; however, the results are different from gold standard. Based on the results shown in Fig. 6 and 7, our method is sensitive to parameters such as threshold, curvature, SE dilation size, number of parts in the narrow volume. According to fig 5 and fig 6 the best result obtained when threshold is 0.003 and the curvature parameter is 0.005. Smoothing coefficient controls the result smoothness. If it is large, we lose the prominent edges. If the smoothing coefficient is small, the result is not smooth enough.

V. Conclusion

In this paper, we proposed a new method to segment liver in CT images. The main innovation of our method includes definition of a local speed map to solve problems of low-contrast images and leakage into nearby tissues. It achieved better results compared to recent and conventional levelset segmentation techniques.

In future, we consider applying our method on more datasets including liver images with more tumors and include shape information in the energy function.

VI. References

[1] Lee, J., Kim, N., Lee, H., Seo, J. B., Won, H. J., Shin, Y. M., ... & Kim, S. H. (2007). Efficient liver segmentation using a level-set method with optimal detection of the initial liver boundary from level-set speed images. Computer methods and programs in biomedicine, 88(1), 26-38.

978-1-5386-3609-1/17/$31.00 ©2017 IEEE

[2] Chan, T.F. and L.A. Vese, Active contours without edges. IEEE Transactions on image processing, 2001. 10(2): p. 266-277.

[3] X.-F. Wang, H. Min, A level set based segmentation method for images with intensity inhomogeneity, LNAI 5755, ICIC, 2009. 670–679.

[4] Pluempitiwiriyawej, C., et al., STACS: New active contour scheme for cardiac MR image segmentation. IEEE transactions on medical imaging, 2005. 24(5): p. 593-603.

[5] Foruzan, A. H., Chen, Y. W., Zoroofi, R. A., Furukawa, A., Sato, Y., Hori, M., & Tomiyama, N. (2013). Segmentation of liver in low-contrast images using K-means clustering and geodesic active contour algorithms. IEICE TRANSACTIONS on Information and Systems, 96(4), 798-807.

[6] E96–D (2013) 798–807.Witkin, A., D. Terzopoulos, and M. Kass, Signal matching through scale space. International Journal of Computer Vision, 1987. 1(2): p. 133-144.

[7] Caselles, V., R. Kimmel, and G. Sapiro, Geodesic active contours. International journal of computer vision, 1997. 22(1): p. 61-79.

[8] Yang, X., et al., A hybrid semi-automatic method for liver segmentation based on level-set methods using multiple seed points. Computer methods and programs in biomedicine, 2014. 113(1): p. 69-79.

[9] Wang, X.-F., et al., A novel level set method for image segmentation by incorporating local statistical analysis and global similarity measurement. Pattern Recognition, 2015. 48(1): p. 189-204.

[10] X.-F. Wang, H. Min, A level set based segmentation method for images with intensity inhomogeneity, LNAI 5755, ICIC, 2009. 670–679.

[11] Jiang, X., R. Zhang, and S. Nie, Image segmentation based on level set method. Physics Procedia, 2012. 33: p. 840-845.

[12] Caselles, V., et al., A geometric model for active contours in image processing. Numerische mathematik, 1993. 66(1): p. 1-31.

[13] Mumford, D. and J. Shah, Optimal approximations by piecewise smooth functions and associated variational problems. Communications on pure and applied mathematics, 1989. 42(5): p. 577-685.

[14] Pluempitiwiriyawej, C., et al., STACS: New active contour scheme for cardiac MR image segmentation. IEEE transactions on medical imaging, 2005. 24(5): p. 593-603

[15] Dong, F., Z. Chen, and J. Wang, A new level set method for inhomogeneous image segmentation. Image and Vision Computing, 2013. 31(10): p. 809-822.

[16] Osher, S. and J.A. Sethian, Fronts propagating with curvature-dependent speed: algorithms based on Hamilton-Jacobi formulations. Journal of computational physics, 1988. 79(1): p. 12-49.

[17] Wang, L., et al., Active contours driven by local Gaussian distribution fitting energy. Signal Processing, 2009. 89(12): p. 2435-2447.

978-1-5386-3609-1/17/$31.00 ©2017 IEEE